

SUPPORTING INFORMATION

DLS and XPS characterisation of PEGylated polymer nanocarriers: internal structure and surface properties

Edvige Celasco^{1,2}, Ilaria Valente², Daniele L. Marchisio^{2*}, Antonello A. Barresi²

¹Dipartimento di Fisica, Università di Genova

via Dodecaneso 33

16146 Genova, Italy

²Dipartimento di Scienza Applicata e Tecnologia (DISAT), Politecnico di Torino

C.so Duca degli Abruzzi 24

10129 Torino, Italy

Corresponding author: Daniele L. Marchisio (daniele.marchisio@polito.it)

Supporting information contents

Materials and methods

Nanosphere and nanocapsule preparation

Figure A1. CIJM geometry and size details.

DLS characterization

XPS characterization – sample preparation

XPS characterization – spectra acquisition and interpretation

Morphology analysis by FESEM

Results and discussion

Influence of feed conditions, quenching and solvent evaporation on nanocapsule size

Figure A2. Influence of feed conditions (in terms of the average velocity of the fluid in the inlet jets) on the mean size of non-quenched and quenched nanocapsules.

Figure A3. Mean nanospheres size for particulate systems obtained with mixer of different scale, for non-quenched and quenched samples.

Figure A4. Influence of feed conditions and quench on nanocapsules size.

Zeta potential characterization of NS and NC

Figure A5. Measured zeta potential for quenched and non-quenched NS and NC obtained with different MR.

In-depth chemical analysis of NS and NC with Argon gun

Figure A6. Atomic percentage for NS and NC versus sputter time obtained with the Argon gun.

Angle-resolved XPS analysis of NS and NC

Figure A7. Atomic concentration versus $\sin(\theta)$ for NS and NC obtained with AR-XPS.

FESEM analysis of nanoparticles

Figure A8. Image of particles obtained with FESEM.

Materials and methods

Nanosphere and nanocapsule preparation

NS and NC were prepared through solvent-displacement. In this method the copolymer is dissolved in an organic solvent (acetone in our case) and the solution is mixed with an antisolvent (water) wherein the solvent is miscible but not the copolymer, which as a consequence precipitates in the form of NS. In NC also the oil is dissolved in the acetone solution, and when the two liquids are mixed the copolymer precipitates around the droplets of oil.

Mixing of the solvent and antisolvent streams was realized using a Confined Impinging Jet Mixer. CIJM consists of two high velocity linear jets of fluid that collide inside a small chamber, whose size affects the global mixing rate. Being the overall process influenced by mixing, its use in nanoparticle preparation processes was proven to be very effective. A sketch of the CIJM used in this work is reported in Figure A1.

4 mL of each of the two solutions of solvent (acetone) and antisolvent (water), charged into two plastic syringes, were pumped into the CIJM by a syringe pump (KDS200, KD Scientific) and collected into a beaker.

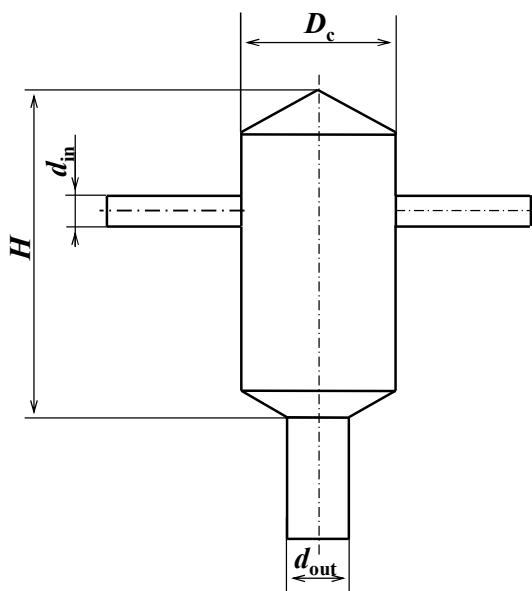


Figure A1. CIJM geometry and size details: chamber diameter, $D_c = 4.8 d_{in}$; outlet diameter, $d_{out}=2 d_{in}$; chamber height, $H=11.2 d_{in}$.

DLS characterization

The Zetasizer Nanoseries ZS90 from Malvern Instrument, employed for DLS characterization, measures both the particle size distribution and the zeta potential. Particle size is measured accurately in the range between 2 nm and 1000 nm. The light beam source is located with a 90° angle with respect to the detector. It allows to analyse samples as suspension without further preparation. The instrument measures the intensity of scattered light as a function of time: since smaller particles move faster than bigger ones, the intensity of scattered light changes with time. From this variation the diffusion coefficient is calculated and then inserted in the Stoke-Einstein equation, which allows to calculate the mean particle size and the polydispersity index (PDI) and to reconstruct the underlying particle size distribution (by assuming a Gaussian functional form).

The zeta potential is determined by measuring the electrophoretic mobility of particles in suspension through the Smoluchowski theory. The zeta potential is the electric potential around the particle at the so-called “shear-plane”. In fact, a charged particle in suspension attracts ions from the bulk solution of opposite sign, creating the so-called Stern layer. The following layers will contain ions of both signs, with a predominance of those opposite to the surface charge.

XPS characterization – sample preparation

Samples for the XPS analyses were prepared as follows. A homogeneous drop of NS and NC suspension was deposited on a silicon substrate, dried for one day in a desiccator and, after this procedure, was left untouched for 12 hours in the XPS pre-chamber, under vacuum conditions, in order to outgas all the volatile components. Before the XPS characterization the surface was mapped with a FESEM-like image (SXI secondary X-ray generated image) in order to sample an homogeneous area. Silicon is used here as substrate since its peaks have binding energies very different from those of the copolymer.

XPS characterization – spectra acquisition and interpretation

XPS is a spectroscopic technique, in which samples are irradiated with X-rays, under ultra-high vacuum conditions, and the kinetic energy and the number of electrons, escaping the top 1 to 10 nm of the sample, measured.

XPS analyses are carried out in this work with a VersaProbe5000 (Physical Electronics) Scanning ESCA Microprobe. The spectra obtained, counts of photo-electrons emitted for second (c/s) versus energy binding (eV), were acquired with the Summit 1.3.6 software, and the fitting procedure was carried out with the Multipak software (v.9.2). Further mathematical treatments (i.e., deconvolution) needed in some specific cases were performed with the Multipak software (v. 9.0) and with the standard Shirley background subtraction.

Standard procedures for the atomic percentage calculations were employed. The atomic concentration (AC) calculations provided the ratio of each component to the sum of the other components.

Morphology analysis by FESEM

In the morphological analysis by Field Emission Scanning Electron Microscopy (Zeiss Gemini Auriga), the charging effect was contained by using an acceleration voltage of 3 kV (possible range 0.1-30kV) and an aperture size of 30 μm of diameter with an InLens detector. A chromium thin film was deposited, on the surface, before the FESEM characterization, in order to reduce charging effects induced to the copolymer.

Results and discussion

Influence of feed conditions, quenching and solvent evaporation on nanocapsule size

Fig. A2 shows an example of the influence of the inlet flow rate, and thus of the inlet jet velocity, on the final nanocapsule size, for the $MR = 1.26$ and an initial copolymer concentration of 6 mg/mL, with and without quenching.

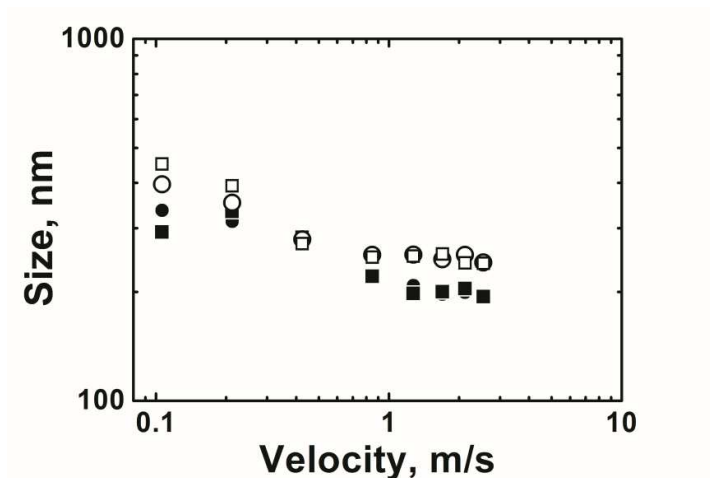


Figure A2. Influence of feed conditions (in terms of the average velocity of the fluid in the inlet jets) on the mean size of non-quenched (open symbols) and quenched nanocapsules (filled symbols) at inlet polymer concentration 6 mg/mL and $MR=1.26$; sample before (circle symbols) and after (square symbols) solvent evaporation are shown.

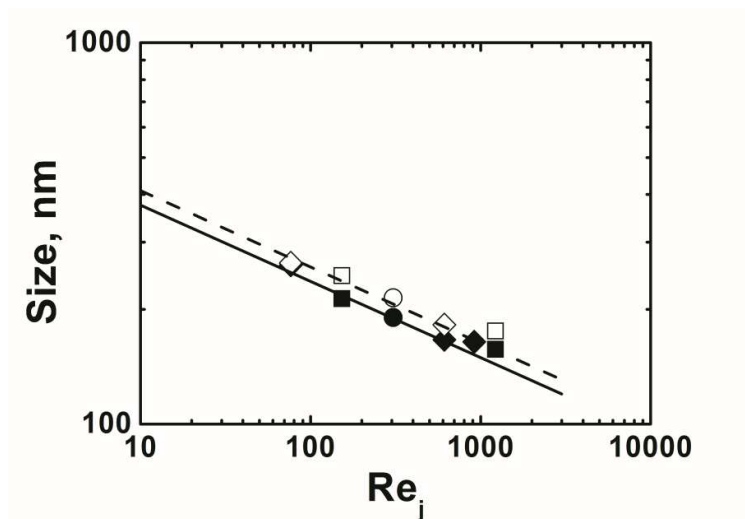


Figure A3. Mean nanospheres size for particulate systems obtained with scale-down (squares), CIJM-d1 (diamonds), scale up (circles) mixer; non-quenched (open symbols) and quenched samples (filled symbols) at inlet polymer concentration 6 mg/mL.

In the same figure both the size before and after solvent evaporation are shown, for the different operating conditions. It appears that solvent evaporation does not affect considerably the final NC mean size, especially at higher flow rates and when operating with quench; the behaviour is similar

for nanospheres. The differences between the pre- and the post-evaporation measurements fall inside the experimental uncertainty, which is about 30 % when working without quenching (but with a large difference between low flow rates and high flow rates) and around 16 % when working with quenching.

Figure A3 shows the influence of the feed velocity for nanospheres; in this case data obtained in mixer of different size are compared. The results show that for geometrically similar mixing devices, the inlet jet Reynolds number is able to correlate the data obtained at different inlet flow rates.

Figures A2 and A3 also show the effect of quench, that is of fast dilution at the exit of the mixer; in the case of nanospheres, quenched samples are only slightly smaller (maximum difference is lower than 10%), but it is interesting to observe that the behaviour is not influenced by the operating conditions (i.e., jet Reynolds number).

For the NC, the influence of quench is generally stronger and seems to depend on MR (see Fig. A4). For $MR = 1.26$, in fact, the data show that the non-quenched samples are about 40% larger (and this value is almost independent of Re_j). At different MR values quite different behaviours are observed: not only the relative size increase is strongly related to MR, but also the dependence on the Reynolds number is reversed. At low MR values the difference in size of quenched and non-quenched NC increases, while at $MR = 2.37$ it decreases when the Reynolds number is increased.

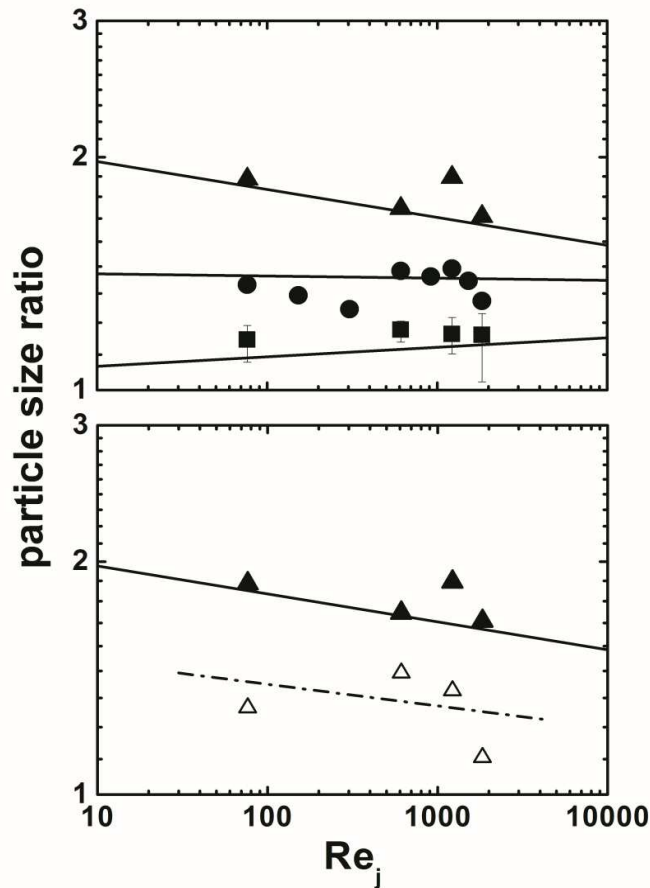


Figure A4. Influence of feed conditions and quench on nanocapsules size.

Non-quenched-to-quenched mean nanocapsule size ratio at different Reynolds numbers and at different MR and copolymer concentrations (■ $MR=0.76$ and 4 to 10 mg/mL copolymer; ● $MR=1.26$, 6 mg/mL copolymer, 8 μ L/mL oil; ▲ $MR=2.37$, 6 mg/mL copolymer, 15 μ L/mL; bottom: △ $MR=2.37$, 3.2 mg/mL copolymer, 8 μ L/mL).

The data in Figure A4 (upper graph) refer to the same copolymer concentration (6 mg/mL), with the exception of those at MR=0.76: in this case the copolymer concentration has been varied in the range 4 to 10 mg/mL, and the averaged data with deviation bars are shown, confirming that at low MR not only the size increase is comparable to that of nanospheres, but also that only the polymer/oil concentration is relevant, and not their absolute concentration.

In the bottom graph of Fig. A4 the results obtained at the same MR=2.37 but at different absolute concentrations are compared, showing that when the oil fraction increases also the absolute concentration of oil and copolymer is influent; in this case in fact, the size vs. Re_j relationship has the same exponent, but the value of the relative size increase is significantly different; it is interesting to note that while at this MR value larger nanocapsules are obtained with smaller polymer concentration, both in quenched and non-quenched conditions, the relative increase in the two cases is significantly smaller than with lower MR values investigated.

Zeta potential characterization of NS and NC

No clear trend is detectable either for NS and NC when the zeta potential of different samples is correlated with the mean size, as shown in Fig. A5. As clearly visible, the zeta potential seems to be independent from the operating conditions and quenching seems to have very little effect. However, although significant differences in the value of the zeta potential are not observed, as it has been shown in this work, the surface structure of NS differ from that of NC.

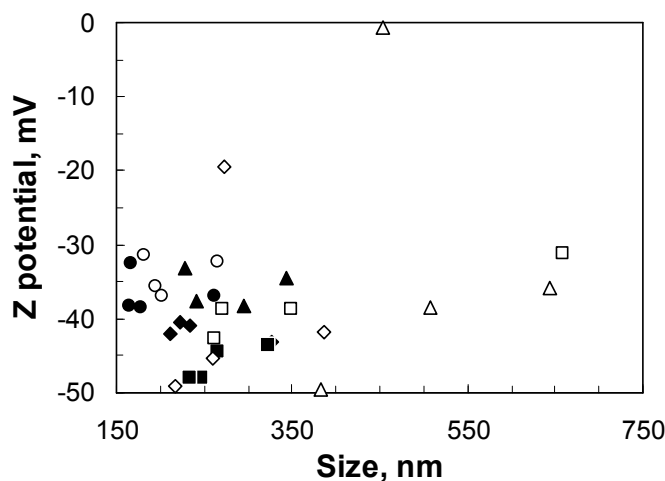


Figure A5. Measured zeta potential for quenched (filled symbols) and non-quenched (open symbols) NS (circles) and NC obtained with MR = 0.76 (diamonds), 1.26 (squares), 2.37 (triangles).

In-depth chemical analysis of NS and NC with Argon gun

For completeness and comparison purposes the results obtained with Argon gun, adopted during the preliminary investigation, are reported. As already mentioned Argon ions can break the C–O bonds of the polymeric chains, due to the interaction with smaller dimension of the Argon ion, and consequently the information relative to these investigations can be distorted. The experimental results, showed in Fig. A6, compared with those obtained with the C60 gun, evidence that the Argon ion gun cannot be employed for the investigation of this kind of polymeric materials.

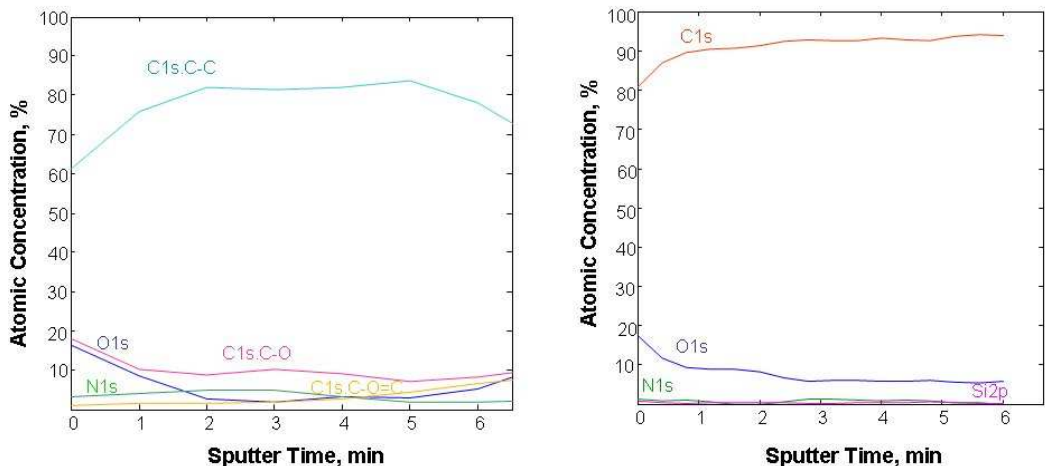


Figure A6. Atomic percentage for NS (left) and NC (right) versus sputter time (min) obtained with the Argon gun.

Angle-resolved XPS analysis of NS and NC

The results of this analysis are reported in Fig. A7 where the derived atomic concentrations are plotted versus the sine of the tilting angle, θ .

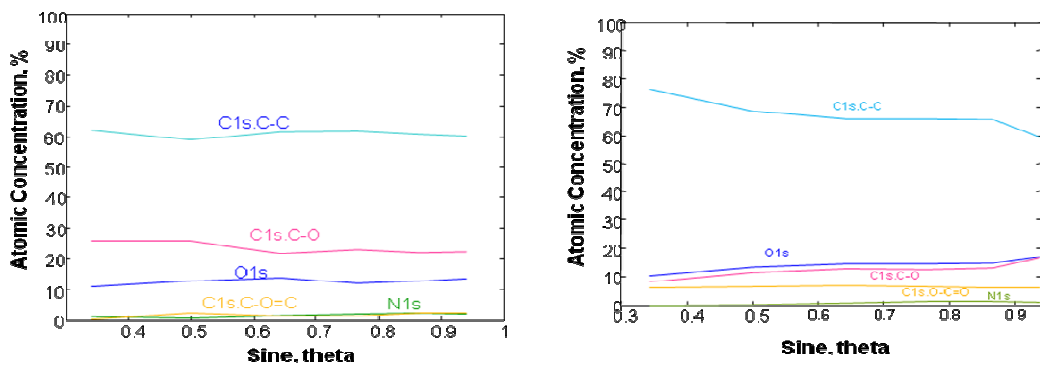


Figure A7. Atomic concentration versus $\sin(\theta)$ for NS (left) and NC (right) obtained with AR-XPS.

FESEM analysis of nanoparticles

FESEM characterization was also carried out to confirm the size of the nanoparticles with a direct method.

The secondary electron image, give us a morphologic informations of our sample in good agreement with our suggestion and interpretation.

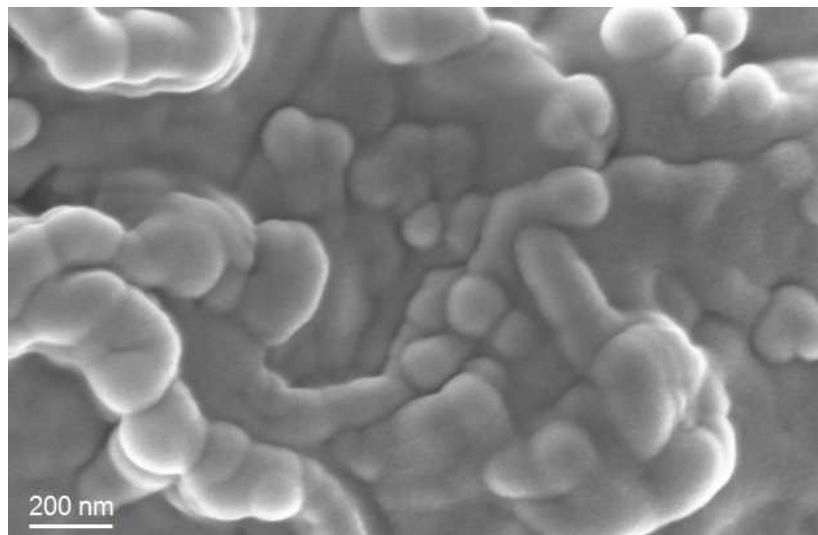


Figure A8. Image of particles with size ranging approximately from 120 to 190 nm obtained with FESEM.